Decreased IRS Signaling Impairs β-Cell Cycle Progression and Survival in Transgenic Mice Overexpressing S6K in β-Cells

Lynda Elghazi,[1] Norman Balcazar,[1] Manuel Blandino-Rosano,[1] Corentin Cras-Méneur,[1] Szabolcs Fatrai,[1] Aaron P. Gould,[1] Maggie M. Chi,[2] Kelle H. Moley,[2] and Ernesto Bernal-Mizrachi[1]

OBJECTIVE—The purpose of this study was to evaluate the role of the S6K arm of mammalian target of rapamycin complex 1 (mTORC1) signaling in regulation of β-cell mass and function. Additionally, we aimed to delineate the importance of in vivo S6K activation in the regulation of insulin signaling and the extent to which alteration of insulin receptor substrate (IRS) signaling modulates β-cell mass and function.

RESEARCH DESIGN AND METHODS—The current experiments describe the phenotype of transgenic mice overexpressing a constitutively active form of S6K under the control of the rat insulin promoter.

RESULTS—Activation of S6K signaling in these mice improved insulin secretion in the absence of changes in β-cell mass. The lack of β-cell mass expansion resulted from decreased G_1-S progression and increased apoptosis. This phenotype was associated with increased p16 and p27 and decreased Cdk2 levels. The changes in cell cycle were accompanied by diminished survival signals because of impaired IRS/Akt signaling.

CONCLUSIONS—This work defines the importance of S6K in regulation of β-cell cycle, cell size, function, and survival. These experiments also demonstrate that in vivo downregulation of IRS signaling by TORC1/S6K induces β-cell insulin resistance, and that this mechanism could explain some of the abnormalities that ultimately result in β-cell failure and diabetes in conditions of nutrient overload. *Diabetes* 59:2390–2399, 2010

Pancreatic β-cells expand their function and mass in both physiologic and pathologic states of nutrient excess and increased insulin demand. Failure of β-cells to expand adequately in settings of increased insulin demand results in hyperglycemia and diabetes. The mechanisms involved in β-cell failure in diabetes are not well understood, but determining how glucose and fat overload lead to impaired β-cell mass and function is a key component for understanding the natural history of diabetes and generating pharmacologic agents to treat and prevent this disease.

The mammalian target of rapamycin (mTOR) signaling pathway integrates growth factors and nutrient signals and is essential for cell growth and proliferation (1,2). This pathway is negatively regulated by the activation of tuberous sclerosis complex TSC1/2 and AMP-activated protein kinase (AMPK) signaling pathways (3–7). The mTOR is part of two distinct complexes: mTORC1 and mTORC2. The mammalian TORC1 is sensitive to rapamycin and regulates protein translation modulation of ribosomal S6 kinase (S6K), eukaryote initiation factor 4E binding protein 1 (4E-BP1), and eukaryote initiation factor 4E (eIF4E) (8). The mTORC1 is composed of regulatory associated protein of mTOR (Raptor), mLst/GβL, deptor and proline-rich PKB/Akt substrate 40 kDa (PRAS40). The mTORC2 complex includes Lst8/GβL, deptor, rapamycin-insensitive companion of mTOR (Rictor), proline-rich protein 5 (PRR5), and stress-activated protein kinase-interacting protein-1 (mSIN) (9,10). The effects of mTORC1 signaling on cell growth, cell size, and cell cycle progression are mediated, at least in part, by phosphorylation of the downstream effectors S6K and 4E-BP1 (11). Activation of S6K by mTOR phosphorylates the ribosomal protein S6 (rpS6). The importance of S6K signaling in β-cells has been assessed in genetically modified models. Global S6K1 knockouts or mice with knockin at all five phosphorylatable serine residues of rpS6 exhibit decreased β-cell mass, impaired insulin secretion, and hyperglycemia (12,13). Moreover, S6K is important for insulinoma formation induced by activation of Akt signaling (14). A major limitation for understanding the role of S6K signaling in β-cells using S6K-deficient mice is the concomitant alteration in insulin sensitivity by negative feedback on insulin receptor substrate (IRS) proteins (15–17). In contrast, activation of mTORC1 signaling by conditional deletion of TSC2 in β-cells enhances β-cell mass as a result of increased proliferation and cell size (18,19). These experiments suggest that mTORC1/S6K signaling is an important regulator of β-cell mass, although the molecular mechanisms and downstream signaling pathways are not well characterized.

Growing evidence suggests that not only fat consumption, but also protein intake and an increase in plasma amino acid concentration, contribute to the development of glucose intolerance, insulin resistance, and type 2 diabetes (20,21). Recent findings demonstrate that S6K activation in states of nutrient overload modulates insulin sensitivity by negatively regulating IRS1 function under conditions of nutrient overload (15–17,22). In addition, the 4E-BP1/eIF4E signaling pathway regulates glucose metabolism by modulation of sensitivity to diet-induced obesity and insulin resistance (23). Although this evidence underscores the importance for mTOR/S6K activation in peripheral tissues as a central player
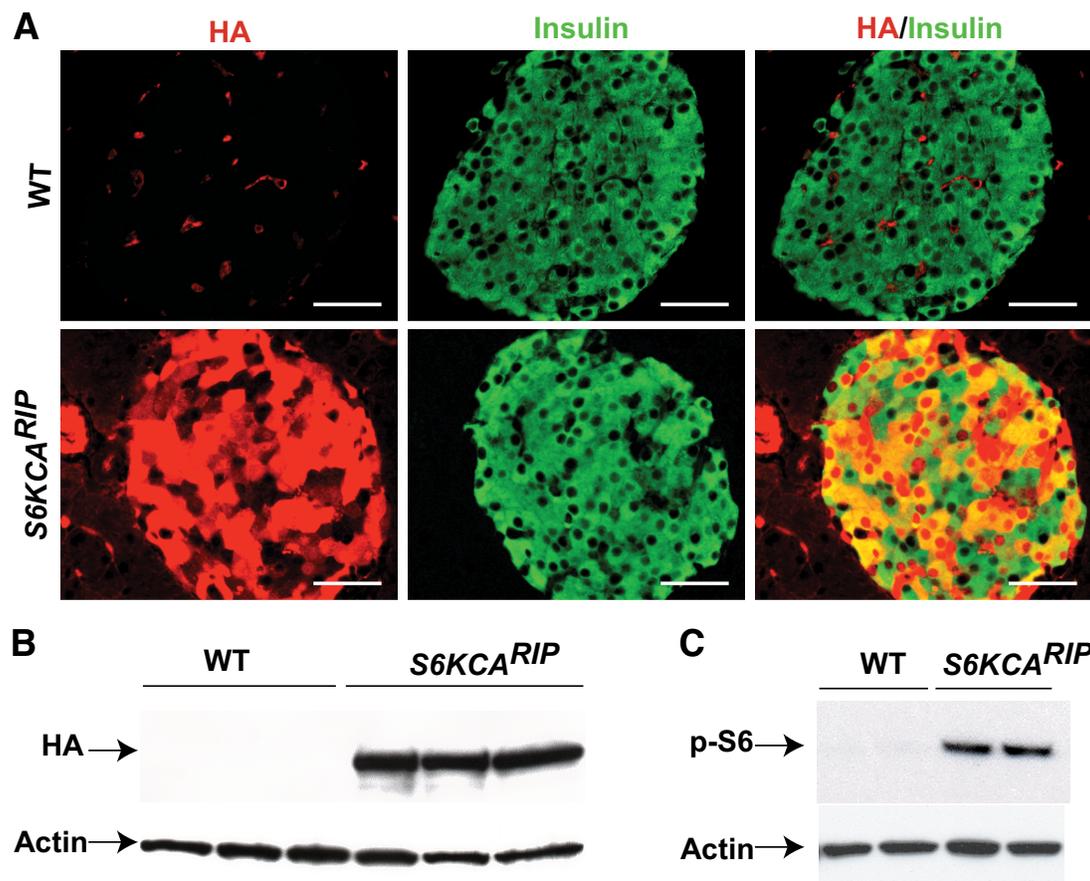
FIG. 1. Assessment of transgene expression and activity in $S6KCA^{RIP}$ and wild-type (WT) mice. *A*: Staining for HA-tag (red) and insulin (green) of pancreatic sections from 3-month-old wild-type and $S6KCA^{RIP}$ mice. *B*: Immunoblotting for HA-tag in islet lysates from 3-month-old wild-type and transgenic mice. *C*: S6 kinase activity was assessed by immunoblotting for phospho-S6 protein using islets from wild-type and $S6KCA^{RIP}$ animals cultured overnight in 2 mmol/l glucose, 2% serum. Immunoblotting for actin was used as loading control. The figures are representative blots of at least three independent experiments, all in duplicate ($n \geq 6$). Scale bars represent 25 μm. (A high-quality digital representation of this figure is available in the online issue.)

in insulin resistance in nutrient overload, the consequences of activation of this pathway in pancreatic β-cells and the implication of the negative feedback inhibition on IRS signaling in vivo are unknown.

To study the role of S6K activation in β-cells, we developed transgenic mice overexpressing a constitutively active form of S6K in β-cells ($S6KCA^{RIP}$). $S6KCA^{RIP}$ mice exhibited improved glucose tolerance because of an increase in insulin secretion and without changes in β-cell mass. The lack of β-cell expansion was characterized by a failure of β-cells to progress normally through the cell cycle and increased apoptosis. Interestingly, these alterations resulted, at least in part, by feedback inhibition on IRS1/2/Akt signaling and increased levels of p16 and p27. The current work defines the importance of the S6K arm activation of mTORC1 signaling in regulation of β-cell cycle, cell size, function, and survival. These experiments also demonstrate that in vivo downregulation of IRS signaling by TORC1/S6K reduces growth factor signaling, and this mechanism could explain some of the abnormalities that ultimately result in β-cell failure and diabetes in conditions of nutrient overload.

RESULTS

$S6KCA^{RIP}$ mice have increased S6 kinase activity in islet β-cells. To increase S6K signaling in β-cells, we inserted a rapamycin-resistant p70S6K Δ2–46/ΔCT104

(T412E) downstream of the rat insulin I promoter ($S6KCA^{RIP}$) (24). Three viable and fertile lines were obtained, and offspring from two founders with similar transgene expression and disturbances in glucose tolerance were studied. The current studies describe the phenotypic characterization of one of these lines. Transgene expression assessed by immunostaining for hemagglutinin (HA) showed cytoplasmic and nuclear staining in most of the β-cells (~80–90%) from $S6KCA^{RIP}$ mice (Fig. 1*A*). Immunoblotting for HA also displayed expression of the transgene exclusively in $S6KCA^{RIP}$ (Fig. 1*B*). Transgene expression was 4.6-fold higher than that of endogenous S6K ($P < 0.05$). S6K activity measured by phosphorylation of rpS6 was increased in $S6KCA^{RIP}$ mice (Fig. 1*C*).

$S6KCA^{RIP}$ mice exhibit improved glucose tolerance and enhanced insulin secretion. Glucose levels in 6-h fasted $S6KCA^{RIP}$ mice were lower than those of wild-type mice (Fig. 2*A*). $S6KCA^{RIP}$ mice exhibited higher insulin values than wild-type mice after 6-h fasting (Fig. 2*A*). No difference in glucose was observed after overnight fasting (time 0; Fig. 2*B* and *C*, and data not shown). Glucose tolerance test in 4-month-old $S6KCA^{RIP}$ mice showed lower glucose levels at 30 and 60 min (Fig. 2*B*). Improved glucose tolerance was observed in 4- and 18-month-old $S6KCA^{RIP}$ mice (data not shown and Fig. 2*C*), indicating that these mice were protected from the impaired glucose tolerance associated with aging (Fig. 2*C*). No changes in
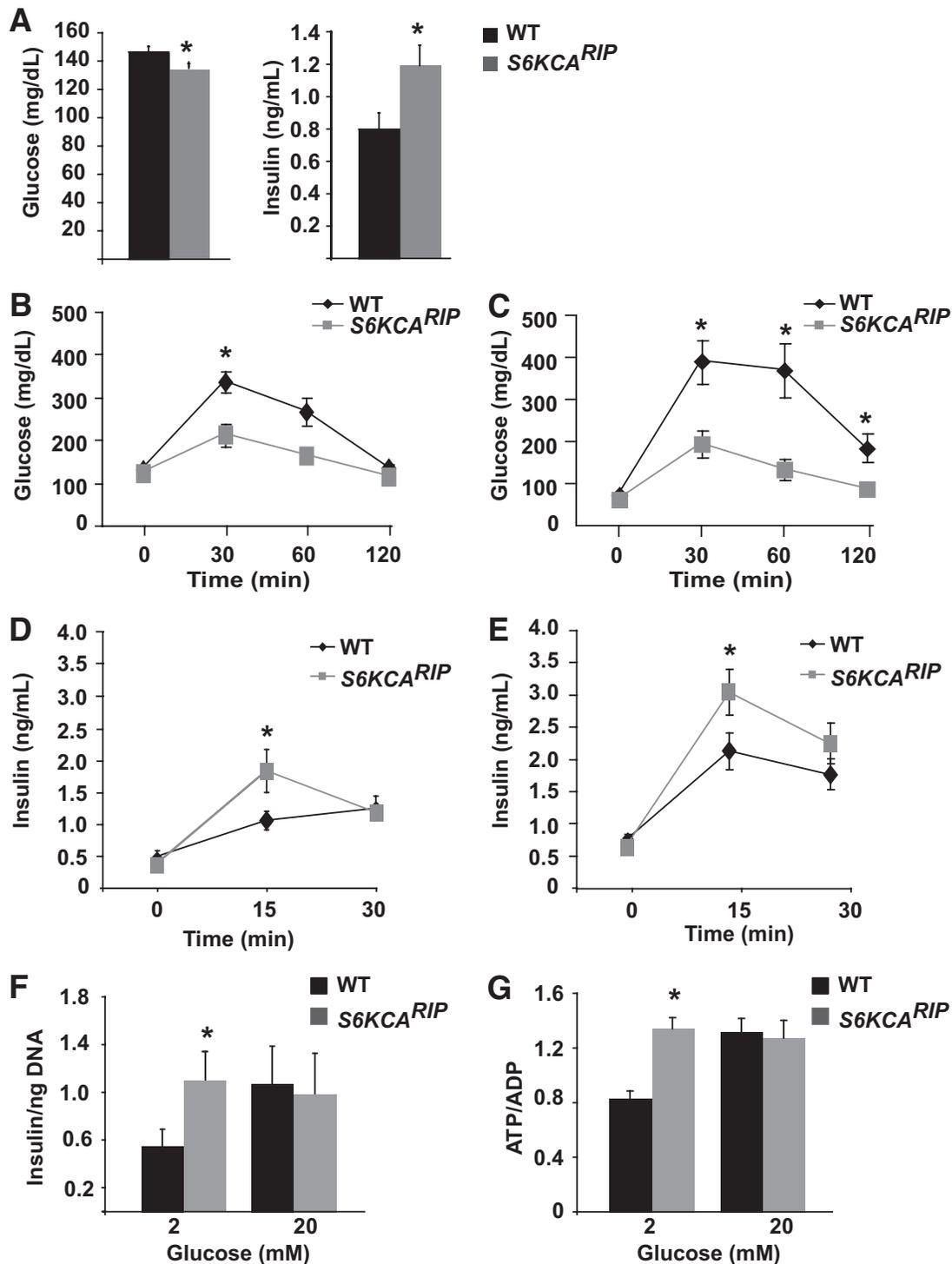
FIG. 2. *S6KCA^RIP* exhibit improved glucose tolerance and augmented glucose-stimulated insulin secretion. *A*: Glucose and insulin levels in 4-month-old wild-type (WT) and *S6KCA^RIP* male mice after 6 h of fasting (*n* = 12). Intraperitoneal glucose tolerance tests were performed in 4- (*B*) and 18- (*C*) month-old wild-type and *S6KCA^RIP* male mice. In vivo insulin secretion after intraperitoneal glucose in wild-type and *S6KCA^RIP* mice at 4 (*D*) and 18 (*E*) months of age. *F*: Insulin secretion in isolated islets assessed by static incubation. *G*: Measurement of ATP/ADP ratio in isolated islets. Data are presented as mean of ATP/ADP ratio per islet from at least 20 islets per mouse (*n* ≥3). In vivo data are presented as mean ± SE (**P* < 0.05; *n* ≥6).

insulin sensitivity were observed by insulin tolerance tests (data not shown).

Glucose-stimulated insulin secretion demonstrated comparable insulin values after overnight fasting in 4- and 18-month-old *S6KCA^RIP* and wild-type mice (Fig. 2*D* and *E*). Insulin levels at 15 min after glucose injection were increased in 4- and 18-month-old *S6KCA^RIP* mice (Fig. 2*D*

and *E*). No difference between *S6KCA^RIP* mice and controls were observed after 30 min of glucose injection (Fig. 2*D* and *E*). Static incubation of isolated islets demonstrated increased insulin levels in islets from *S6KCA^RIP* mice when exposed to 2 mmol/l glucose (Fig. 2*F*). Insulin secretion was comparable after stimulation with 20 mmol/l glucose (Fig. 2*F*). Measurements of ATP/ADP content in
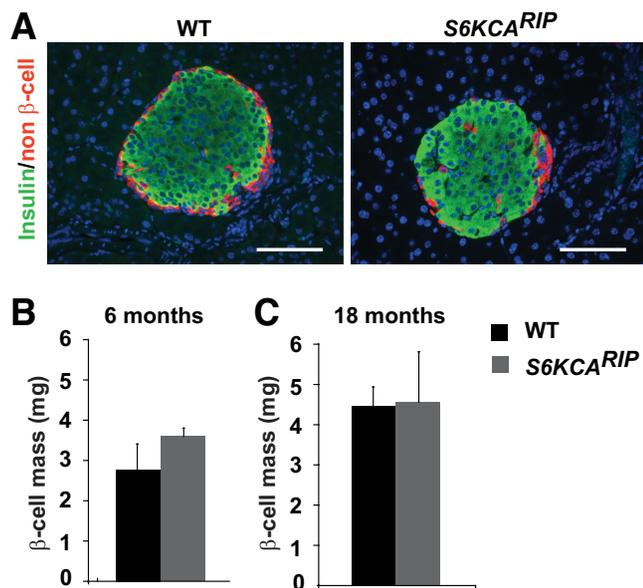
FIG. 3. Islet morphometry in wild-type (WT) and *S6KCA*^{RIP} animals. *A*: Immunofluorescence staining for insulin (green) and non–β-cells (red) in pancreatic sections from wild-type and *S6KCA*^{RIP} mice. Assessment of β-cell mass in 6- (*B*) and 18- (*C*) month-old wild-type and *S6KCA*^{RIP} male mice. Data are presented as mean ± SE (*P < 0.05; $n \geq 3$). Scale bars represent 25 μm. (A high-quality digital representation of this figure is available in the online issue.)

isolated islets showed that islets from *S6KCA*^{RIP} mice exhibited higher levels of ATP/ADP in 2 mmol/l glucose (Fig. 2*G*). Similar ATP/ADP levels between wild-type and *S6KCA*^{RIP} were obtained with 20 mmol/l glucose.

Islet morphometry and analysis of cell size. Immunofluorescence staining for insulin and non–β-cells showed that islet architecture was conserved in *S6KCA*^{RIP} mice (Fig. 3*A*). Similar β-cell mass between *S6KCA*^{RIP} and wild-type mice β-cells was comparable at 6 and 18 months of age (Fig. 3*B* and *C*). Islet size distribution between *S6KCA*^{RIP} and wild-type mice was unchanged (data not shown). Double staining for HA and insulin in dispersed islets from *S6KCA*^{RIP} and wild-type mice showed that β-cells from transgenic mice appeared to have increased in size (supplementary Fig. 1 in the online appendix available at http://diabetes.diabetesjournals.org/cgi/content/full/db09-0851/DC1). Cell size measurements in pancreatic sections stained for Glut2 and HA demonstrated a 50% increase in the size of β-cells expressing the transgene (Fig. 4*A* and *B*, P < 0.05). The number of β-cells per islet was reduced in *S6KCA*^{RIP} mice, suggesting that islets from these mice exhibited fewer β-cells with increased cell size (Fig. 4*C*, P < 0.05).

Assessment of proliferation and apoptosis in *S6KCA*^{RIP} and wild-type mice. β-Cell proliferation assessed by Ki67 staining showed increased proliferative rate in *S6KCA*^{RIP} mice (Fig. 5*A*). The increased proliferative rate with absence of changes in β-cell mass suggests that β-cells failed to complete the cell cycle or underwent programmed cell death. Since Ki67 is a marker for G1, G2, S, and M phases, we used bromodeoxyuridine (BrdU) and phospho-Histone-3 (pH3) to specifically assess cell cycle progression through the S and M phases, respectively. The rate of BrdU in β-cells was similar between *S6KCA*^{RIP} and wild-type mice, indicating that β-cells were not progressing to the S phase (Fig. 5*B*). Also, no difference in the rate of pH3 in β-cells was observed between wild-type and
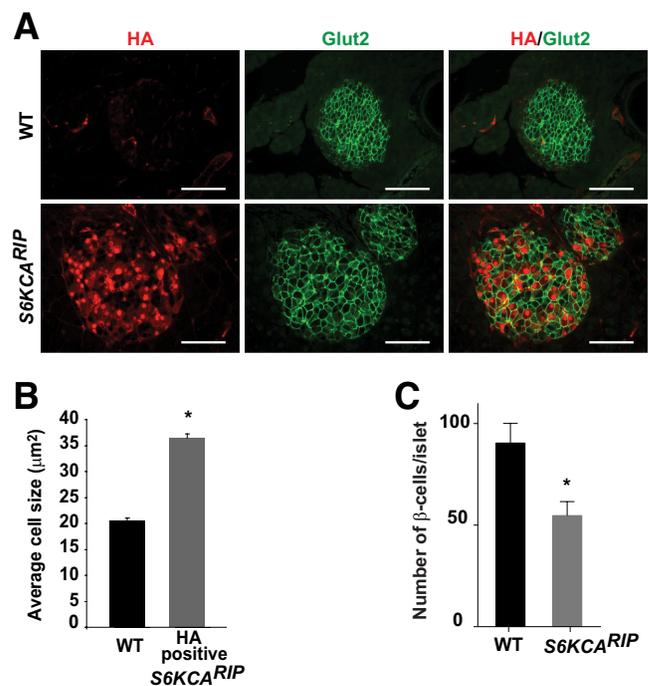
FIG. 4. Assessment of β-cell size in wild-type (WT) and *S6KCA*^{RIP} animals. *A*: Pancreatic section from wild-type and *S6KCA*^{RIP} mice were immunostained for HA (red) and Glut2 (green). *B*: Quantitation of β-cell size in islets from wild-type and *S6KCA*^{RIP} mice. Cell size in β-cells from *S6KCA*^{RIP} mice is presented based on expression of the transgene (HA positive). Data include measurements of at least 250 cells from 4 wild-type and *S6KCA*^{RIP} mice. *C*: Number of β-cells per islet was calculated in at least 80 islets from wild-type and *S6KCA*^{RIP} mice. Data are presented as mean ± SE (*P < 0.05; $n \geq 3$). Scale bars represent 25 μm. (A high-quality digital representation of this figure is available in the online issue.)

S6KCA^{RIP} mice (data not shown). Assessment of β-cell apoptosis by cleaved caspase 3 staining showed a fourfold increase in apoptosis in *S6KCA*^{RIP} mice (Fig. 5*C*). Similar increases in apoptosis in *S6KCA*^{RIP} mice were observed by using transferase-mediated dUTP nick-end labeling (TUNEL) assay (Fig. 5*D*). The results of these experiments suggest that increased S6K activity in β-cells induced entry, but delayed completion of the cell cycle. In addition, these mice also exhibited increased apoptosis.

Alterations in cell cycle progression in *S6KCA*^{RIP} mice are associated with increased p27 and p16 levels. Assessment of cell cycle components responsible for G_1-S progression demonstrated that protein levels for Cyclin D1, D2, D3, E, and Cdk4 were similar in islets from *S6KCA*^{RIP} and wild-type mice (Fig. 6*A*). In contrast, Cdk2 was reduced in islets from *S6KCA*^{RIP} mice (Fig. 6*A*). Levels for p16, a major regulator of G_1-S progression in β-cells, were increased in islets from *S6KCA*^{RIP} mice (Fig. 6*A*). Assessment of the Cip/Kip inhibitors p21 and p27 showed that p27 levels were higher in *S6KCA*^{RIP} mice (Fig. 6*A*). The number of β-cells with nuclear p27 was increased in *S6KCA*^{RIP} mice (Fig. 6*B*).

Decreased IRS signaling in β-cells from *S6KCA*^{RIP} transgenics. To determine whether islets from *S6KCA*^{RIP} mice exhibited decreased IRS/Akt signaling, we performed immunostaining for phospho-GSK3β. Marked reduction of phospho-GSK3β staining was observed in islets from *S6KCA*^{RIP} mice (Fig. 7*A*). Levels for IRS1 and IRS2 were decreased by 50 and 40%, respectively, in islet lysates from *S6KCA*^{RIP} mice (Fig. 7*B*, P < 0.05). Phosphorylation of IRS1 on Ser 307, one of the many S6K phosphorylation sites on
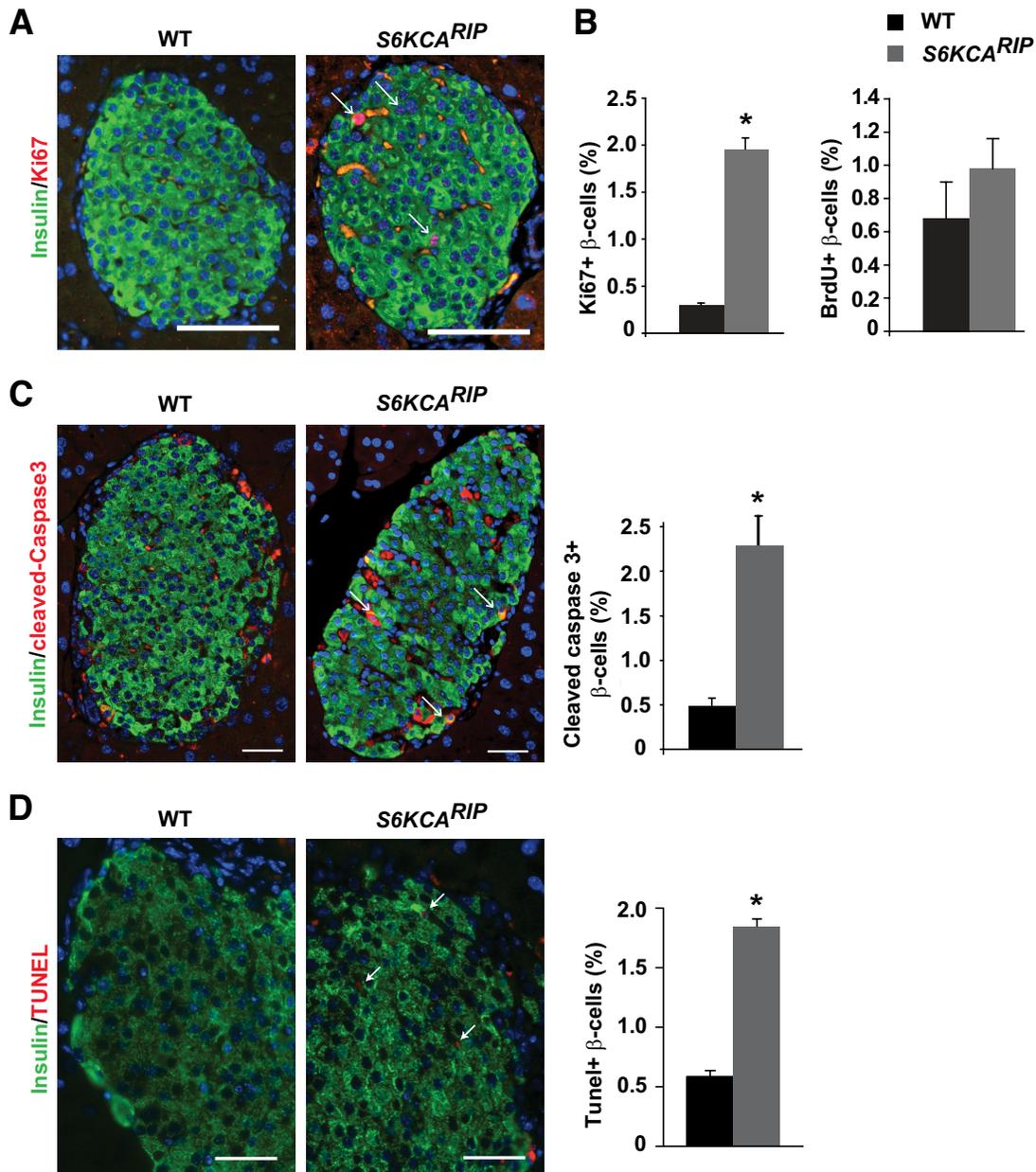
FIG. 5. Assessment of β-cell proliferation and apoptosis in wild-type (WT) and *S6KCA^RIP* mice. *A*: Proliferative index in sections stained for Ki67 and insulin (*arrows*: double positive cells). *B*: Proliferative rate on sections stained for BrdU and insulin. Quantitation of apoptosis by immunostaining for cleaved caspase 3 (*C*) and TUNEL assay (*D*) in insulin-stained sections (apoptotic rate). β-Cells positive for cleaved caspase 3 and TUNEL are marked with *arrows*. Data are presented as mean ± SE (*$P < 0.05$; $n \geq 3$). Scale bars represent 25 μm. (A high-quality digital representation of this figure is available in the online issue.)

IRS1, was increased in *S6KCA^RIP* mice (Fig. 7*B*). The decreased IRS1 and IRS2 levels were associated with decreased levels of phospho-GSK3β and phospho-FoxO1 in islets from *S6KCA^RIP* mice (Fig. 7*B*). As expected reduced Akt signaling also resulted in increased TSC2 levels in *S6KCA^RIP* mice (Fig. 7*B*). We next assessed the alterations in IRS/Akt signaling after stimulation with insulin-like growth factor 1 (IGF1) (Fig. 7*C*). Phosphorylation of Akt at Ser473 was unchanged in *S6KCA^RIP* mice (Fig. 7*C*). *S6KCA^RIP* mice exhibited reduction of Akt phosphorylation at Thr308. The decreased phosphorylation of Akt at Thr308 resulted in reduced Akt activity, as demonstrated by phosphorylation of GSK3β (Fig. 7*C*). Interestingly, phosphorylation of 4E-BP1, a downstream mTORC1 target, was reduced in *S6KCA^RIP* mice. The results of the current experiments demonstrate

that activation of S6K in β-cells reduces Akt activity by decreasing the levels of IRS proteins.

DISCUSSION

The results of the current studies serve to elucidate the importance of S6K in regulation of β-cell mass and function and provide insight into the molecular mechanisms involved in the adaptation of β-cells to states of nutrient overload and hyperglycemia. Similar to exposure of β-cells to glucose and amino acids, activation of S6K signaling resulted in improved glucose tolerance, insulin secretion, and hyperinsulinemia. These findings show, for the first time, that activation of S6K induces β-cell insulin resistance by feedback inhibition of IRS signaling. Importantly,
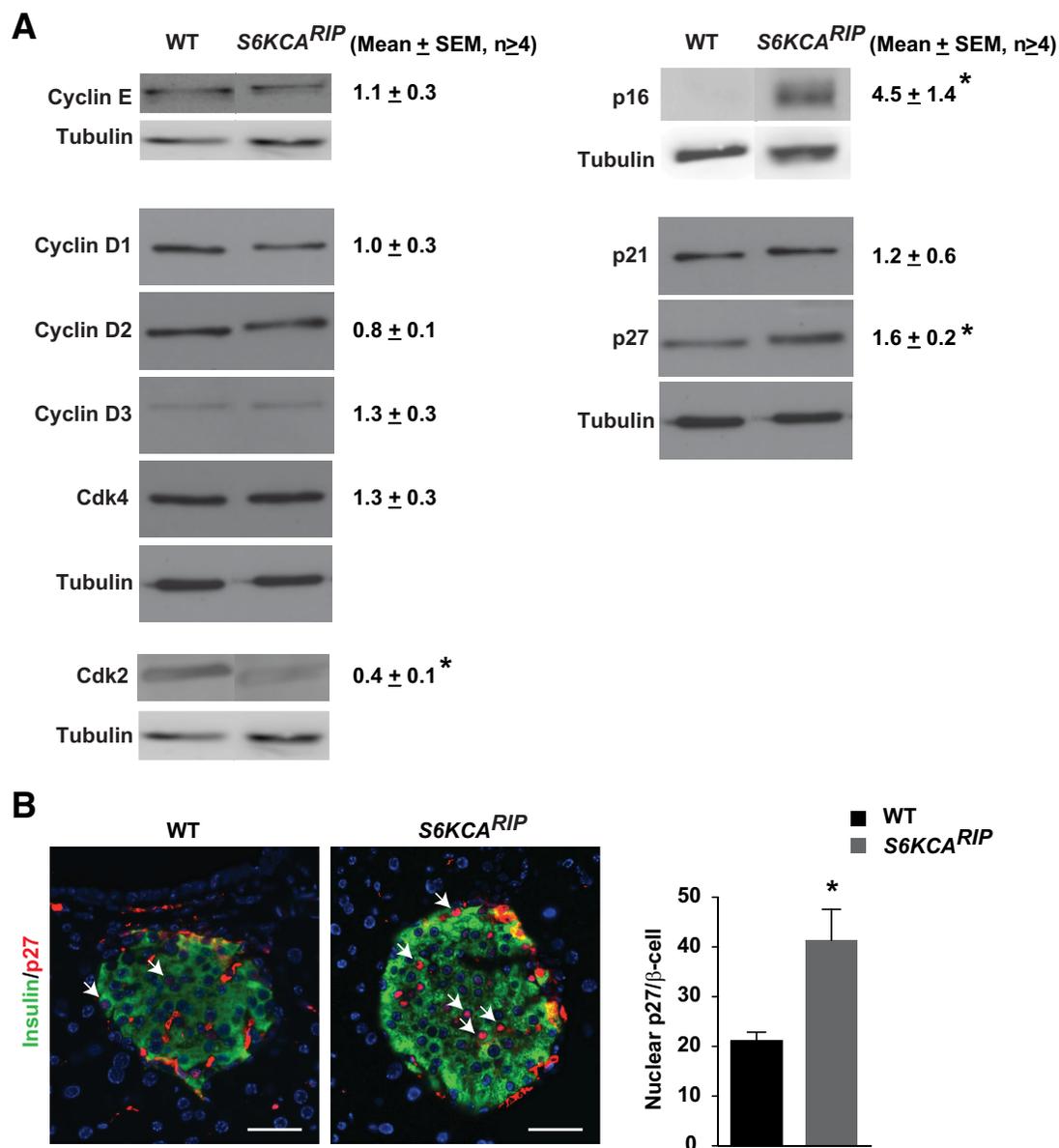
FIG. 6. Assessment of cell cycle components in wild-type (WT) and *S6KCA*[RIP] mice. *A*: Immunoblotting for cyclin/Cdk complexes using islet lysates from wild-type and *S6KCA*[RIP]. Densitometric analysis of protein bands for cyclin/Cdk complex components in islet lysates from 4-month-old wild-type and *S6KCA*[RIP] mice is presented next to each immunoblot. The figures are representative blots of at least three experiments, all in duplicate (*$P < 0.05$; $n \geq 6$). *B*: Quantitation of nuclear p27 in β-cells (*arrows*) from wild-type and *S6KCA*[RIP] mice ($n \geq 3$). At least 2,000 β-cells were included in the analysis. Data are presented as mean ± SE (*$P < 0.05$). Scale bars represent 25 μm. (A high-quality digital representation of this figure is available in the online issue.)

these studies also show that S6K regulates IRS2 levels, a major determinant for β-cell proliferation and survival. The β-cell insulin resistance induced by this mechanism had major effects on cell cycle regulation by modulation of Cdk2, p27, and p16 levels. Another major effect of insulin resistance in this model was the increased apoptosis by decreased survival signals from Akt. The current work suggests that one of the major consequences of chronic exposure of β-cells to nutrient overload is the development of impaired IRS signaling. These results serve to elucidate some of the abnormalities observed in adaptive responses of β-cells to nutrient excess and tentatively to explain some of the mechanisms involved in glucose toxicity. Finally, these data also demonstrate that the negative feedback of S6K on IRS signaling can be a major modulator of β-cell mass and function in vivo.

The current study shows that activation of S6K signaling in β-cells causes improved glucose tolerance by increase in insulin secretion. The augmented insulin secretion in the presence of normal β-cell mass suggests that S6K modulates glucose-induced insulin secretion. Based on the insulin secretion experiments, it is possible that S6K activation regulates early events in insulin secretion, and islet perifusion experiments will be required to address this. The mechanism involved in this process is not completely understood, but our experiments suggest that modulation of the ATP/ADP ratio could play an important role. Similar to the potentiation of insulin secretion by amino acids reported in the literature, the maximal increase in ATP/ADP ratio observed in islets from S6K in low glucose could prime β-cells to respond to a glucose challenge (25). These findings together with impaired
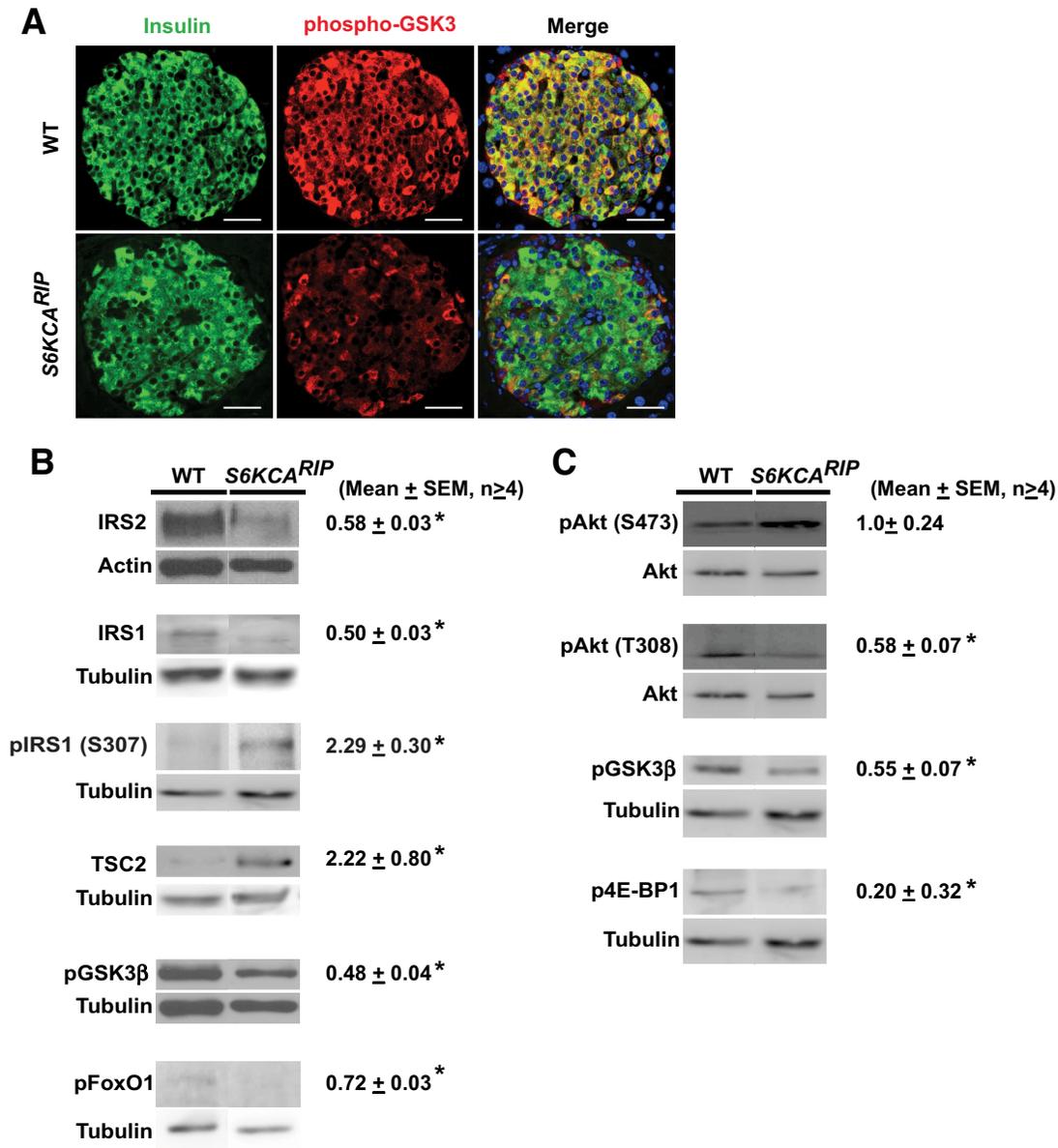
FIG. 7. Immunoblotting for IRS/Akt signaling components in wild-type (WT) and *S6KCA^{RIP}* mice. *A*: Immunofluorescence staining using anti-phospho-GSK3 (red) and insulin (green) in pancreatic sections from wild-type and *S6KCA^{RIP}* mice. *B*: Immunoblotting and quantitation for different components of IRS/Akt signaling in islet lysates from wild-type and *S6KCA^{RIP}* mice. Scanning densitometry of protein bands and quantitation is presented next to the respective immunoblot ($n \geq 4$). Immunoblotting for actin or tubulin were used as loading control. Quantitation of the data are presented as percentage of the control ($n = 4$). *C*: Assessment of phosphorylation of Akt, GSK3β, and 4E-BP1 in islet from wild-type and *S6KCA^{RIP}* mice after stimulation with IGF1 (100 nmol/l) for 15 min ($n \geq 4$). Data are presented as mean ± SE (*$P < 0.05$). Scale bars represent 25 μm. (A high-quality digital representation of this figure is available in the online issue.)

glucose tolerance and defective insulin secretion in S6K1-deficient mice or mice with knock-in at serine residues of rpS6 suggest that S6K modulates insulin secretion. The mechanism implicated in defective insulin secretion in these models is unclear, but previous evidence suggests that small cell size with a reduction in membrane surface has pronounced effects on insulin secretion (26,27). The relation between cell size and insulin secretion is intriguing, and it is reasonable to speculate that increased cell size and membrane surface size could contribute to the augmented insulin secretion observed in *S6KCA^{RIP}* mice. Further studies are needed to evaluate this hypothesis and to explore a role of S6K in regulation of distal exocytotic events involved in first and second phases of insulin secretion.

In the present work, overexpression of S6K recapitulated the proliferative and the cell size phenotype described in mice overexpressing a constitutively active form of Akt and mice with conditional deletion of TSC2 in β-cells (18,28,29). These results suggest that this kinase relates some of the proliferative and growth signals induced by Akt/mTOR. The effect of S6K on β-cell proliferation is also in agreement with recent findings implicating this kinase in insulinoma formation by Akt activation (14). The absence of β-cell mass changes, together with the results of Ki67, BrdU, and pH3 measurements, suggests that more β-cells enter the cell cycle, but G_1-S progression is delayed by partial inhibition of the cyclin D/Cdk4 and cyclin E/Cdk2 complexes. The alteration in G_1-S progression could be explained in part by increased levels of p16

and p27, respectively, and lower Cdk2 expression. The normal β-cell mass in this model could be explained by a balance between increased entry, but slow progression through the cell cycle combined with increased apoptosis and a long half-life of β-cells. The increase in p16 levels is intriguing, as this cell cycle inhibitor is a biomarker of aging and is elevated in aged β-cells (30). It is possible that continuous activation of S6K reproduces some of the abnormalities observed in aged β-cells. The augmented levels and nuclear localization of p27 observed in $S6KCA^{RIP}$ mice were most likely caused by a negative feedback inhibition in IRS/Akt signaling. The decreased insulin/IRS/Akt signaling could alter p27 levels by several mechanisms, including FoxO1-mediated p27 transcription (31,32) and/or increases in p27 stability by GSK3β (33). Decreased IRS signaling induces nuclear p27 in β-cells from IRS2-deficient mice (34). The importance of p27 in regulation of the β-cell cycle in our model resembles the findings obtained in islets from models of diet-induced obesity and suggests that S6K signaling may be implicated in the β-cell failure observed in this model (34). Based on the current studies and published evidence, p27 levels are likely to be a marker for impaired IRS signaling in β-cells. This mechanism plays a pivotal role in regulating cell-cycle progression under normal conditions or in states of β-cell expansion (34). A major difference between the β-cell mass phenotype of $βTSC2^{-/-}$ and $S6KCA^{RIP}$ mice is that β-cells from $βTSC2^{-/-}$ are probably less susceptible to inhibition in IRS signaling, as the mTOR activation in this model is downstream and not dependent on IRS signaling. In addition, the activation of the mTORC2/Akt pathway could activate survival signals.

The alteration of β-cell survival was the other major component observed by augmented S6K signaling in β-cells. The mechanism involved in apoptosis in these mice could be multifactorial, but our results are consistent with a critical role for a negative feedback of S6K on IRS1/IRS2/Akt signaling. The decreased Akt activity was characterized by decreased phosphorylation of Thr308, but not Ser473, suggesting alterations in PDK1 and not mTORC2 activity. Assessment of downstream Akt targets in islets from $S6KCA^{RIP}$ mice implied that the inhibition of IRS2/Akt signaling observed in $S6KCA^{RIP}$ induced apoptosis by activation of FoxO1 and GSK3β. Interestingly, Pdx1 levels in $S6KCA^{RIP}$ mice were unchanged, suggesting that this is not a major contributor to the increased apoptosis in these mice (data not shown). The inhibition of IRS signaling by S6K-mediated phosphorylation and degradation of IRS1 signaling has been demonstrated in vivo and in vitro (15–17). Less is known about a feedback inhibition on IRS2 signaling, but recent data on INS1 cells suggest that IGF1 signaling downregulates IRS2 protein by activation of mTOR signaling (35). Our results show, for the first time, that S6K regulates IRS2 levels in vivo, and that this mechanism has major implications for regulation of survival and cell cycle progression in β-cells. The increased apoptosis observed in $S6KCA^{RIP}$ mice was unexpected, as S6K has been shown to induce pro-survival signals by inhibiting BAD in lymphocytes (36). This discrepancy could be explained by the fact that β-cells are very sensitive to modulation of IRS2 levels, as demonstrated in mice deficient for IRS2 (37). The decreased survival in the S6K mice is in contrast to the absence of apoptosis in $βTSC2^{-/-}$ mice (18). These could be explained, at least in part, by the antiapoptotic effects induced by activation of the eIF4E and mTORC2 activation (21,38,39). Taken to-

gether, these studies suggest that β-cell insulin resistance induced by a negative feedback of S6K on IRS signaling not only affects cell cycle progression, but also impairs survival signals. However, activation of S6K signaling alone is not sufficient to induce β-cell failure and diabetes.

The results of the current studies suggest that activation of S6K could play a major role in regulation of β-cell cycle progression and function, and implies that S6K relates proliferative but not survival pathways induced by Akt signaling or activation of mTORC1 signaling. Another important conclusion from these studies is that activating proliferation is not always associated with increases in mass, and that therapeutic strategies should include pharmacologic agents that alter proliferation and apoptosis. These studies collectively show the importance of the S6K arm of mTOR signaling in regulating proliferation, cell size, function, and survival, and increase our knowledge about the mechanism used by β-cells to regulate G_1-S transition and mass. Additionally, these studies provide information about the adaptation of the β-cell to states of nutrient overload.

EXPERIMENTAL PROCEDURES

Generation of transgenic mice. The S6K mutant used in these studies contains deletion of amino acids 2–46, truncation of carboxy-terminal 104 amino acids, and threonine to glutamatic acid mutation at position 412 (p70S6K ΔD2–46/ΔDCT104 T412E). This mutant confers rapamycin resistance and increases in basal S6K activity in transfected cells (24,40). To achieve overexpression of a constitutively active form of S6K in β-cells, this construct was inserted behind the rat insulin promoter I ($S6KCA^{RIP}$). Three transgenic founders were obtained and backcrossed to C57BL6J mice, and the N2 and N3 generation from two lines with similar phenotype were analyzed. Wild-type littermate males with comparable mixed background were used as controls for all of the experiments. All procedures were performed in accordance with Washington University's Animal Studies Committee and the University Committee on Use and Care of Animals at the University of Michigan.

Metabolic studies. Glucose was measured on whole blood using AccuChek II glucometer (Roche Diagnostics). Plasma insulin levels were determined using a rat insulin ELISA kit (Crystal Chem). Glucose tolerance tests were performed in 12-h fasted animals by injecting glucose (2 g/kg) intraperitoneally as described (28). Insulin secretion in vivo was assessed using 3 g/kg of glucose intraperitoneally in overnight-fasted mice.

Islet studies. Islet isolation was accomplished by collagenase digestion as described previously (28). Insulin secretion was assessed by static incubation of isolated islets as described (41). After overnight culture in RPMI containing 5 mmol/l glucose, islets were precultured for 1 h in Krebs-Ringer medium containing 2 mmol/l glucose. Groups of 10 islets in triplicate were incubated in Krebs-Ringer medium containing 2 mmol/l glucose or 20 mmol/l glucose for 1 h.

For ATP and ADP measurements, islets were isolated and cultured for 24 h in RPMI containing 5 mmol/l glucose. Thereafter, islets of similar size were handpicked and precultured for 1 h in 0.5 ml Krebs-Ringer medium without glucose in an organ-culture dish. Groups of 20 islets were incubated for 1 h in Krebs-Ringer containing 2 mmol/l and 20 mmol/l glucose, respectively, and rinsed three times in

Ringer without glucose. Individual islets were hand picked in 1-μl medium, placed on a slide, and frozen immediately in 2-methylbutane prechilled with liquid nitrogen. They were then freeze-dried at $-35°C$ overnight under vacuum with less than 0.01 mm of Hg and removed for extraction. Each islet was extracted in 0.5 μl of 0.1 N NaOH under oil, heated at 80°C for 20 min, and neutralized with a 0.2-μl mixture of 0.2 mol/l HCl and 0.1 mol/l TrisHCl pH6.8. Samples were stored at $-80°C$. Aliquot (0.1 μl) was obtained for ATP and ADP microanalysis respectively (42). Data are presented as mean of ATP/ADP ratio per islet from at least 20 islets per mouse. For the experiments using IGF1, islets were serum deprived for an hour followed by stimulation with IGF1 (100 nmol/l) for 15 min.

Immunofluorescence staining. Pancreatic tissues were fixed overnight in 3.7% formalin and embedded in paraffin using standard techniques. The following antibodies were used: guinea pig anti-insulin (Dako), mouse anti-HA.11 (Covance), rabbit anti-glucagon (Chemicon), rabbit anti-pancreatic polypeptide (Chemicon), rabbit antisomatostatin (Dako), rabbit anti-Glut2 (a gift from Bernard Thorens), rabbit anti-Ki67 (Vector), rabbit anti-cleaved caspase 3 (Cell Signaling), rabbit anti-phospho-GSK3α/β (Ser21/9) (Cell Signaling), mouse anti-BrdU (Amersham), and mouse anti-p27^{Kip1} (BD Transduction). TUNEL assays were performed using the ApopTag Plus fluorescein in situ apoptosis detection kit (Chemicon). The fluorescent secondary antibodies were from Jackson Laboratories. DAPI (Vector) was used to counterstain nuclei.

Western blotting. Protein from islet lysates were run in polyacrylamide gels and transferred to polyvinylidene fluoride membranes. Protein-band densitometry was determined using the same membrane by pixel intensity using NIH Image J software (v1.42 freely available at http://rsb.info.nih.gov/ij/index.html) (43) and normalized against that of actin or tubulin. Antibodies used for immunoblotting are included in supplementary Table 1.

Islet morphometry. The β-cell mass was calculated by point-counting morphometry from 5 insulin-stained sections (5 μm) separated by 200 μm using the BQ Classic98 MR software package (BIOQUANT) as described (28). Cell size was determined in immunofluorescence-stained sections for Glut2 and HA. Sectioned areas of individual β-cells from wild-type and transgenic mice that were HA positive were measured using NIH Image J software (v1.42) (43). The number of β-cells per islet was calculated by dividing the number of β-cells in at least 80 islets per animal. Proliferation was assessed in sections stained with insulin and Ki67, BrdU, and phospho-Histone-3. At least 3,000 insulin-stained cells were counted for each animal. Apoptotic rates were determined using cleaved caspase 3 and TUNEL assay (ApopTag Red In Situ Apoptosis Detection Kit, Chemicon) in insulin-stained sections. At least 2,000 β-cells were counted in a blinded fashion.

Statistical analysis. All values are expressed as mean $\pm$ SEM. For all other comparisons, paired Student t test was used. Differences were considered statistically significant at $P < 0.05$.

REFERENCES

1. Wullschleger S, Loewith R, Hall MN. TOR signaling in growth and metabolism. Cell 2006;124:471–484
2. Um SH, D'Alessio D, Thomas G. Nutrient overload, insulin resistance, and ribosomal protein S6 kinase 1, S6K1. Cell Metab 2006;3:393–402
3. Manning BD, Tee AR, Logsdon MN, Blenis J, Cantley LC. Identification of the tuberous sclerosis complex-2 tumor suppressor gene product tuberin as a target of the phosphoinositide 3-kinase/akt pathway. Mol Cell 2002; 10:151–162
4. Inoki K, Li Y, Zhu T, Wu J, Guan KL. TSC2 is phosphorylated and inhibited by Akt and suppresses mTOR signalling. Nat Cell Biol 2002;4:648–657
5. Zhang Y, Gao X, Saucedo LJ, Ru B, Edgar BA, Pan D. Rheb is a direct target of the tuberous sclerosis tumour suppressor proteins. Nat Cell Biol 2003;5:578–581
6. Garami A, Zwartkruis FJ, Nobukuni T, Joaquin M, Roccio M, Stocker H, Kozma SC, Hafen E, Bos JL, Thomas G. Insulin activation of Rheb, a mediator of mTOR/S6K/4E-BP signaling, is inhibited by TSC1 and 2. Mol Cell 2003;11:1457–1466
7. Inoki K, Li Y, Xu T, Guan KL. Rheb GTPase is a direct target of TSC2 GAP activity and regulates mTOR signaling. Genes Dev 2003;17:1829–1834
8. Harris TE, Lawrence JC Jr. TOR signaling. Sci STKE 2003;2003:re15
9. Sarbassov DD, Ali SM, Kim DH, Guertin DA, Latek RR, Erdjument-Bromage H, Tempst P, Sabatini DM. Rictor, a novel binding partner of mTOR, defines a rapamycin-insensitive and raptor-independent pathway that regulates the cytoskeleton. Curr Biol 2004;14:1296–1302
10. Jacinto E, Loewith R, Schmidt A, Lin S, Ruegg MA, Hall A, Hall MN. Mammalian TOR complex 2 controls the actin cytoskeleton and is rapamycin insensitive. Nat Cell Biol 2004;6:1122–1128
11. Hay N, Sonenberg N. Upstream and downstream of mTOR. Genes Dev 2004;18:1926–1945
12. Shima H, Pende M, Chen Y, Fumagalli S, Thomas G, Kozma SC. Disruption of the p70(s6k)/p85(s6k) gene reveals a small mouse phenotype and a new functional S6 kinase. Embo J 1998;17:6649–6659
13. Ruvinsky I, Sharon N, Lerer T, Cohen H, Stolovich-Rain M, Nir T, Dor Y, Zisman P, Meyuhas O. Ribosomal protein S6 phosphorylation is a determinant of cell size and glucose homeostasis. Genes Dev 2005;19:2199–2211
14. Alliouachene S, Tuttle RL, Boumard S, Lapointe T, Berissi S, Germain S, Jaubert F, Tosh D, Birnbaum MJ, Pende M. Constitutively active Akt1 expression in mouse pancreas requires S6 kinase 1 for insulinoma formation. J Clin Invest 2008;118:3629–3638
15. Um SH, Frigerio F, Watanabe M, Picard F, Joaquin M, Sticker M, Fumagalli S, Allegrini PR, Kozma SC, Auwerx J, Thomas G. Absence of S6K1 protects against age- and diet-induced obesity while enhancing insulin sensitivity. Nature 2004;431:200–205
16. Shah OJ, Wang Z, Hunter T. Inappropriate activation of the TSC/Rheb/mTOR/S6K cassette induces IRS1/2 depletion, insulin resistance, and cell survival deficiencies. Curr Biol 2004;14:1650–1656
17. Harrington LS, Findlay GM, Gray A, Tolkacheva T, Wigfield S, Rebholz H, Barnett J, Leslie NR, Cheng S, Shepherd PR, Gout I, Downes CP, Lamb RF. The TSC1–2 tumor suppressor controls insulin-PI3K signaling via regulation of IRS proteins. J Cell Biol 2004;166:213–223
18. Rachdi L, Balcazar N, Osorio-Duque F, Elghazi L, Weiss A, Gould A, Chang-Chen KJ, Gambello MJ, Bernal-Mizrachi E. Disruption of Tsc2 in pancreatic β cells induces β cell mass expansion and improved glucose

tolerance in a TORC1-dependent manner. Proc Natl Acad Sci U S A 2008;105:9250–9255

19. Shigeyama Y, Kobayashi T, Kido Y, Hashimoto N, Asahara S, Matsuda T, Takeda A, Inoue T, Shibutani Y, Koyanagi M, Uchida T, Inoue M, Hino O, Kasuga M, Noda T. Biphasic response of pancreatic β-cell mass to ablation of tuberous sclerosis complex 2 in mice. Mol Cell Biol 2008;28:2971–2979

20. Krebs M. Amino acid-dependent modulation of glucose metabolism in humans. Eur J Clin Invest 2005;35:351–354

21. Mamane Y, Petroulakis E, LeBacquer O, Sonenberg N. mTOR, translation initiation and cancer. Oncogene 2006;25:6416–6422

22. Tremblay F, Marette A. Amino acid and insulin signaling via the mTOR/p70 S6 kinase pathway. A negative feedback mechanism leading to insulin resistance in skeletal muscle cells. J Biol Chem 2001;276:38052–38060

23. Le Bacquer O, Petroulakis E, Paglialunga S, Poulin F, Richard D, Cianflone K, Sonenberg N. Elevated sensitivity to diet-induced obesity and insulin resistance in mice lacking 4E-BP1 and 4E-BP2. J Clin Invest 2007;117:387–396

24. Weng QP, Kozlowski M, Belham C, Zhang A, Comb MJ, Avruch J. Regulation of the p70 S6 kinase by phosphorylation in vivo. Analysis using site-specific anti-phosphopeptide antibodies. J Biol Chem 1998;273:16621–16629

25. Newsholme P, Bender K, Kiely A, Brennan L. Amino acid metabolism, insulin secretion and diabetes. Biochem Soc Trans 2007;35:1180–1186

26. Giordano E, Cirulli V, Bosco D, Rouiller D, Halban P, Meda P. B-cell size influences glucose-stimulated insulin secretion. Am J Physiol 1993;265: C358–364

27. Swenne I, Crace CJ, Jansson L. Intermittent protein-calorie malnutrition in the young rat causes long-term impairment of the insulin secretory response to glucose in vitro. J Endocrinol 1988;118:295–302

28. Bernal-Mizrachi E, Wen W, Stahlhut S, Welling CM, Permutt MA. Islet β cell expression of constitutively active Akt1/PKB α induces striking hypertrophy, hyperplasia, and hyperinsulinemia. J Clin Invest 2001;108:1631–1638

29. Tuttle RL, Gill NS, Pugh W, Lee JP, Koeberlein B, Furth EE, Polonsky KS, Naji A, Birnbaum MJ. Regulation of pancreatic β-cell growth and survival by the serine/threonine protein kinase Akt1/PKBα. Nat Med 2001;7:1133–1137

30. Krishnamurthy J, Torrice C, Ramsey MR, Kovalev GI, Al-Regaiey K, Su L, Sharpless NE. Ink4a/Arf expression is a biomarker of aging. J Clin Invest 2004;114:1299–1307

31. Medema RH, Kops GJ, Bos JL, Burgering BM. AFX-like Forkhead transcription factors mediate cell-cycle regulation by Ras and PKB through p27kip1. Nature 2000;404:782–787

32. Nakamura N, Ramaswamy S, Vazquez F, Signoretti S, Loda M, Sellers WR. Forkhead transcription factors are critical effectors of cell death and cell cycle arrest downstream of PTEN. Mol Cell Biol 2000;20:8969–8982

33. Surjit M, Lal SK. Glycogen synthase kinase-3 phosphorylates and regulates the stability of p27kip1 protein. Cell Cycle 2007;6:580–588

34. Uchida T, Nakamura T, Hashimoto N, Matsuda T, Kotani K, Sakaue H, Kido Y, Hayashi Y, Nakayama KI, White MF, Kasuga M. Deletion of Cdkn1b ameliorates hyperglycemia by maintaining compensatory hyperinsulinemia in diabetic mice. Nat Med 2005;11:175–182

35. Briaud I, Dickson LM, Lingohr MK, McCuaig JF, Lawrence JC, Rhodes CJ. Insulin receptor substrate-2 proteasomal degradation mediated by a mammalian target of rapamycin (mTOR)-induced negative feedback down-regulates protein kinase B-mediated signaling pathway in β-cells. J Biol Chem 2005;280:2282–2293

36. Harada H, Andersen JS, Mann M, Terada N, Korsmeyer SJ. p70S6 kinase signals cell survival as well as growth, inactivating the pro-apoptotic molecule BAD. Proc Natl Acad Sci U S A 2001;98:9666–9670

37. Withers DJ, Gutierrez JS, Towery H, Burks DJ, Ren JM, Previs S, Zhang Y, Bernal D, Pons S, Shulman GI, Bonner-Weir S, White MF. Disruption of IRS-2 causes type 2 diabetes in mice. Nature 1998;391:900–904

38. Li S, Takasu T, Perlman DM, Peterson MS, Burrichter D, Avdulov S, Bitterman PB, Polunovsky VA. Translation factor eIF4E rescues cells from Myc-dependent apoptosis by inhibiting cytochrome c release. J Biol Chem 2003;278:3015–3022

39. Tan A, Bitterman P, Sonenberg N, Peterson M, Polunovsky V. Inhibition of Myc-dependent apoptosis by eukaryotic translation initiation factor 4E requires cyclin D1. Oncogene 2000;19:1437–1447

40. Alessi DR, Deak M, Casamayor A, Caudwell FB, Morrice N, Norman DG, Gaffney P, Reese CB, MacDougall CN, Harbison D, Ashworth A, Bownes M. 3-Phosphoinositide-dependent protein kinase-1 (PDK1): structural and functional homology with the Drosophila DSTPK61 kinase. Curr Biol 1997;7:776–789

41. Bernal-Mizrachi E, Fatrai S, Johnson JD, Ohsugi M, Otani K, Han Z, Polonsky KS, Permutt MA. Defective insulin secretion and increased susceptibility to experimental diabetes are induced by reduced Akt activity in pancreatic islet β cells. J Clin Invest 2004;114:928–936

42. Lowry OH, Passonneau JV. *A flexible system of enzymatic analysis.* New York, Academic Press, 1972

43. Girish V, Vijayalakshmi A. Affordable image analysis using NIH Image/ImageJ. Indian J Cancer 2004;41:47